IEEE Access
The journal for rapid open access publishing

SPECIAL SECTION ON TOWARD UBIQUITOUS REAL-TIME RADIO PROPAGATION MODELING: THE EXPLOITATION OF CYBER RESOURCES, GPU AND FAST AND ACCURATE EM ALGORITHMS

Received October 1, 2014, accepted October 15, 2014, date of publication October 31, 2014, date of current version November 11, 2014.

Digital Object Identifier 10.1109/ACCESS.2014.2365991

Ray-Tracing-Based mm-Wave Beamforming Assessment

VITTORIO DEGLI-ESPOSTI[1], (Member, IEEE), FRANCO FUSCHINI[1], ENRICO M. VITUCCI[1], (Member, IEEE), MARINA BARBIROLI[1], MARCO ZOLI[1], LI TIAN[2], (Student Member, IEEE), XUEFENG YIN[2], DIEGO ANDRES DUPLEICH[3], ROBERT MÜLLER[3], CHRISTIAN SCHNEIDER[3], AND REINER S. THOMÄ[3], (Fellow, IEEE)

[1]Dipartimento dell'Ingegneria Elettrica e dell'Informazione, Alma Mater Studiorum—Università di Bologna, Bologna 40126, Italy
[2]Channel Research laboratory, Tongji University, Shanghai 200092, China
[3]Ilmenau University of Technology, Ilmenau 98693, Germany

Corresponding author: F. Fuschini (franco.fuschini@unibo.it)

ABSTRACT The use of large-size antenna arrays to implement pencil-beam forming techniques is becoming a key asset to cope with the very high throughput density requirements and high path-loss of future millimeter-wave (mm-wave) gigabit-wireless applications. Suboptimal beamforming (BF) strategies based on search over discrete set of beams (steering vectors) are proposed and implemented in present standards and applications. The potential of fully adaptive advanced BF strategies that will become possible in the future, thanks to the availability of accurate localization and powerful distributed computing, is evaluated in this paper through system simulation. After validation and calibration against mm-wave directional indoor channel measurements, a 3-D ray tracing model is used as a propagation-prediction engine to evaluate performance in a number of simple, reference cases. Ray tracing itself, however, is proposed and evaluated as a real-time prediction tool to assist future BF techniques.

INDEX TERMS MIMO, beamforming, ray tracing, millimeter-wave propagation, channel measurements.

I. INTRODUCTION

Global mobile data traffic is expected to increase 10 times by 2019, and a similar trend is expected for the following years [1]. Wireless data throughput density will probably grow at an even faster rate in dense urban areas and indoor premises, where most of the data is used or generated. In order to cope with this trend, the exploitation of new spectrum in the millimeter-wave (mm-wave) frequency bands as well as advanced radio transmission and antenna techniques, such as massive-MIMO and beamforming (BF) techniques, are being proposed.

A great number of short-range, millimeter-wave applications are being proposed and realized, including gigabit-wireless applications for indoor connectivity [2], wireless back-hauling systems [3], mm-wave transmission for 5G mobile radio [4] and others.

Besides the great free spectrum availability, one of the advantages of mm-wave frequencies is the small wavelength allowing the implementation of compact, massive MIMO antenna arrays and therefore of BF techniques with narrow beams (*pencil-beam forming*) to achieve high spatial-spectrum reuse and signal-to-interference ratios. Moreover, due to the very high through-wall attenuation, the mm-wave indoor channel is usually simpler than the Ultra High Frequency (UHF) channel: it is often a Line-Of-Sight (LOS) or quasi-LOS channel with a few dominant path clusters and a relatively low dense multipath component [5], [6].

The above mentioned characteristics determine a substantial simplification of pencil-beam forming at mm-waves with respect to traditional UHF BF, as the former can simply *address* large-scale directional channel characteristics by steering the beam toward major paths to optimize signal strength and/or by steering zeros toward interfering paths to minimize interference (*direction-based beam forming*). The latter requires more complex channel estimation procedures due to the lower spatial resolution and the greater complexity of the propagation channel [7], [8].

Several strategies can be implemented to determine the directional properties of the channel and to perform pencil-beam forming. Exhaustive search beam-switching techniques have been proposed and included in recent standards such as 802.11ad [9] and 802.15.3c [10], where couples of steering-vectors of a given discrete set are applied in sequence at the transmitter (Tx) and/or at the receiver (Rx) and the corresponding channel is checked for Carrier to Interference plus Noise Ratio (CINR):

the best-performing couple is chosen for transmission. Exhaustive search techniques can be slow when beams are very narrow, and might fail to promptly react upon fast channel changes, e.g. due to abrupt human blockage or terminal movement. Smarter techniques including a preliminary channel sounding phase using larger beams and lower frequencies [11] or iterative methods [12] have been proposed.

In future applications, the progresses of environment digitalization, powerful distributed computing and sensing and localization techniques will allow the development of advanced BF strategies making use of sensing and/or deterministic propagation models such as Ray Tracing (*RT-assisted BF*) to perform real-time prediction of the channel's directional characteristics, thus reducing the need of time-consuming exhaustive search techniques to a minimum. In the simplest case, if accurate localization is available, LOS (or radial) direction BF can be implemented at any time without any necessity for channel sounding.

In this work a full-3D Ray Tracing (RT) simulator including the Effective Roughness scattering model [13] is used as a tool to investigate advanced pencil-beam forming techniques in terms of CINR and throughput density in a reference indoor multi-user environment, where different communications are assumed to be divided through space-division only. The study prescinds from issues related to the practical implementation through exhaustive beam switching techniques, as complete knowledge of the directional characteristics of the channel is assumed. For example a Multi-BF (MBF) technique is proposed where beam-steering is simultaneously performed on the 4 strongest paths and combined with path delay and phase equalization in order to exploit the intrinsic space diversity of the multipath channel and improve robustness vs. abrupt channel changes. Such a technique, due to its intrinsic complexity is only feasible through RT-assisted BF as exhaustive search techniques would result too slow to cope with channel variations.

Therefore 3D RT is used here for system simulation purposes, but the use of RT for real-time, RT-assisted BF is also suggested and briefly discussed at the end of the paper.

The 3D RT model is validated and calibrated using 60 GHz directional measurements in section II, while different BF strategies are introduced in section III and compared through RT simulation in section IV. Real-time, RT-assisted BF potential is discussed in section V, while conclusions are drawn in section VI.

II. RAY BASED MODELLING OF MILLIMETER WAVE PROPAGATION

A. mm-WAVE SOUNDING AND PROPAGATION CHARACTERIZATION

Propagation characteristics at mm-waves differ from the lower bands typically used in communication systems. The main characteristic is its ''quasi-optical'' behavior due to the small wavelength size. Therefore, rough surface scattering effects are enhanced, reflections become more specular-like, and diffraction effects are very small. Path loss is increased due to the high free-space attenuation as suggested by Friis equation [14]. Penetration loss through building materials is significantly higher than at lower bands [15] and limits the indoor communication range mostly to intra-room applications.

The full characterization of propagation properties for channel modelling and RT parameterization requires different propagation path parameters. These include time delay, doppler shift, polarization, Direction of Departure at the Tx (DoD), and Direction of Arrival at the Rx (DoA). However, measuring these parameters jointly can be both expensive and time consuming. A compromise between accuracy and reliability is therefore needed. For example, the use of antenna arrays (challenging to manufacture) with high resolution algorithms can be replaced by the mechanical displacement of single antennas (synthetic arrays), or the rotation of high directive antennas to scan the different DoD and DoA. However, by using synthetic arrays the measurement time is extended and can be applied only to time invariant measurement scenarios. Furthermore, the mechanical movement of the measurement equipment can introduce inaccuracies and systematic errors in measurements. Additionally, the number of scan or angular points is also more frequently lowered to suit reasonably low measurement times.

Although polarization is not always considered in measurements at mm-wave [4] currently found in the literature, it plays an important role to fully characterize propagation characteristics. The small wavelength size amplifies the interaction with scattering structures that change the polarization properties of the waves. A complete polarimetric characterization requires a 3D description of the channel [16]. This is addressed in [17], where a novel channel sounder is also introduced which is capable of coherently measuring polarization properties of propagation at mm-wave.

Within the research community, there are two main approaches in channel sounding: commercially available vector network analyzers (VNA) and custom channel sounders [18], [19]. The VNA is a simple solution, which is typically used in indoor and stationary scenarios. However, due to the greater measurement bandwidth in comparison to lower frequencies, it may be very time consuming to conduct a large number of frequency samples given that this requires longer sweep times. Conversely, custom channel sounders based on wideband pseudo random binary sequence (PRBS), although more expensive, offer shorter measurement times and a high resolution in the time delay domain. This, combined with a high spatial resolution, allows for an easier identification of clusters and paths.

The present measurements were carried out with an ultra-wideband (UWB) channel sounder (CS) developed at the TU Ilmenau [19] (Figure 1). The main features of this system are wideband operation (up to 7 GHz instantaneous bandwidth) and easy scalability of receiver channels. The UWB sounder hardware architecture is based on a base-band M-Sequence radar chip-set [20]. The stimulus signal is a

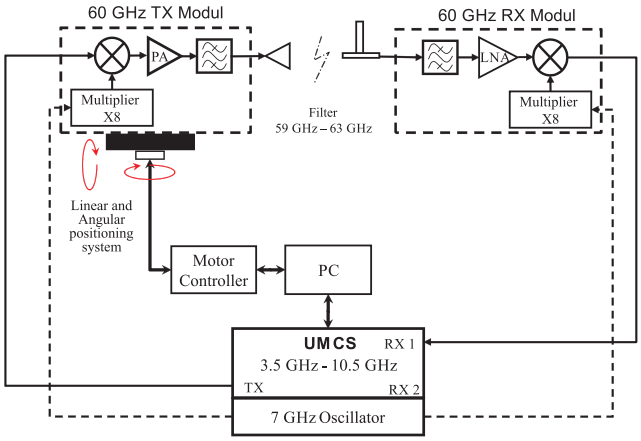

FIGURE 1. Channel sounder setup scheme.

periodic M-Sequence (spread spectrum signal) generated by a high speed 12-stage digital shift register driven by a stable RF-clock generator working at fc = 7 GHz. The frequency range covers measurements in baseband (0 to 3.5 GHz) and FCC-UWB band (3.5 to 10.5 GHz). The M-sequence length is 4095 chips with a sub-sampling frequency of fc/512. This enables a scan rate of about 3300 channel impulse responses per second and per channel. A 60 GHz up/down converter multiplies the 7 GHz clock signal by a factor of 8 to reach the 56 GHz clock used for mixing the FCC-UWB band to reach a range of 59.5 GHz – 63 GHz. After filtering and amplification, the measured bandwidth was reduced to 3 GHz for the 60 GHz band. The maximum output power of the 60 GHz stage is approximately 5 dBm.

FIGURE 2. The "small office" environment.

The measurement scenario was a small office located in the Ilmenau University of Technology (Figure 2). The dimensions, materials, and furniture offer a typical scattering environment for similar scenarios. Even though the results of the measurements correspond to this specific scenario and conditions, they are also valid to be used as reference for the development of stochastic models and parameterization of RT tools. The office was closed during the measurements to guarantee a static environment and time-invariant channel.

The Tx was mounted in a 3D rotating positioner emulating an access point located high in a corner of the room. On the other side, the Rx was fixed over a desk to perform static measurements. The LOS was obstructed on purpose by an absorber, i.e. only reflected and scattered components were captured by the receiver.

A high gain antenna (35 dBi, 5° beam-width) was used at the Tx to offer a high DoD discrimination. The receiver antenna was omni-directional (1.5 dBi). The polarization was changed by rotating 0°/90° sequentially the antennas at both ends, keeping always the phase centre.

The Tx swept a quarter of a sphere, with an angular step of 2° from 0° to 90° in azimuth, and 30° to −60° in elevation, resulting in 2025 measurement points per Tx – Rx polarization combination. Since the environment was static, a total of N = 20 snapshots per measurement point were taken to reduce the noise by averaging. In addition, only the samples 10 dB higher than the noise floor (NF) were kept, discarding the other ones by setting the appropriate channel impulse response (CIR) to zero. In the delay domain, a total of 150 samples were selected, corresponding to a distance of approximately 13 m.

B. RAY TRACING MODEL VALIDATION AND PARAMETRIZATION

Ray Tracing is well known as a graphical rendering technique for producing visual images in 3D environments.

Starting from early nineties RT has been applied also to urban radio propagation, with the main purpose to derive deterministic models for radio channel prediction and mobile radio planning. These models have gained popularity in recent years, thanks to their ability to simulate multipath propagation including the time- and space-dispersion characteristics of the channel, which are important for the design and planning of modern wireless systems. Limitations to their use due to high computation time are being overcome thanks to the increase in computing capacity available in today's computer networks.

RT is based on the Geometrical Theory of Propagation which is an extension of Geometrical Optics (GO) to radio frequencies. As GO, it corresponds to an asymptotic, high-frequency approximation of basic electromagnetic theory, and is based on the ray concept. Since GO does not account for diffraction, the effect of edge and vertex diffraction is taken into account through the so called Geometrical Theory of Diffraction (GTD), or their extension, e.g. the Uniform Theory of Diffraction (UTD) [21]. At mm-wave frequencies GO approximation is less drastic and the propagation environment is more limited due to the high through-wall attenuation, therefore an unprecedented level of accuracy can in theory be achieved.

In this work simulations are performed with a full 3D RT prediction tool, developed at the University of

IEEE Access
The journal for rapid open access publishing

Bologna [13], [22], that takes into account not only reflection, transmission and diffraction, but also Diffuse Scattering (DS) using the Effective Roughness (ER) model [23]. The ER approach allows to simply but effectively describe phenomena related to the roughness of the walls, or to surface/volume irregularities that are not included in the environment representation.

The RT engine requires a detailed description of the geometrical and electromagnetic properties of every object inside the simulated environment, e.g. walls, pieces of furniture, etc. Each object is described in a simplified way as a composition of canonical objects (flat-surface slabs, straight edges, etc.) and for each object the vertex coordinates, the thickness, the complex permittivity and the parameters of the ER diffuse scattering model must be specified. Also the 3D polarimetric radiation characteristics of the Tx and Rx antennas must be given in input to the RT model.

The implemented RT algorithm consists of two main steps: the visibility algorithm and the field computation procedure. The visibility algorithm is the core of the RT simulator, and aims at creating a hierarchical database consisting of the objects and their visibility relations, which are then used to trace the actual ray paths [13].

In the field computation step, for each ray path reflection and transmission losses are computed accordingly to the well-known Fresnel coefficients, the diffraction loss is computed according to the GTD/UTD coefficients, and the effect of diffuse scattering is taken into account through the scattering coefficient S and the scattering diagram, as reported in [23]. In order to satisfy the power balance, the Fresnel coefficient for reflection are reduced according to a proper factor $R = \sqrt{1 - S^2}$, which means that diffuse scattering spreads power in all the directions at the expense of specular reflection. All the interaction types are depicted in Figure 3 with reference to a single wall.

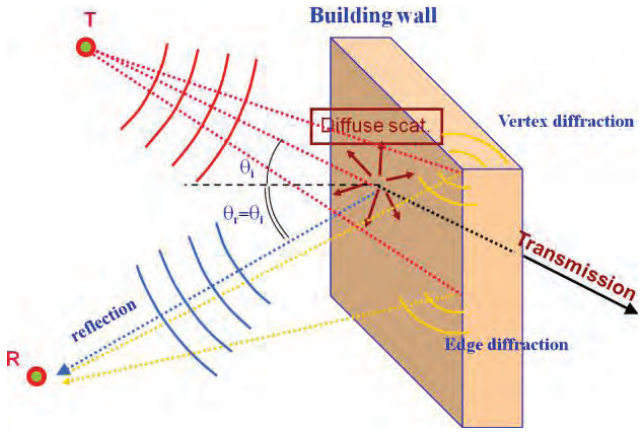

FIGURE 3. Summary of all the possible interaction mechanisms undergone by rays impinging on a single building wall.

Also free-space propagation loss is taken into account to get the total field incident on the Rx antenna. The computation of the total field $\mathbf{E}(Rx)$ at the *Rx* point can be expressed through the following concise formula:

$$\begin{aligned}\mathbf{E}(Rx) &= \sum_{k=0}^{N_R} \mathbf{E}^k(Rx) \\ &= \sum_{k=0}^{N_R} \left\{ \left[\prod_{l=min\left\{1, N_{EV}^k\right\}^=} \mathbf{C}_l \right] \cdot \mathbf{E}_{T0}^k\left(\theta_T{}^k, \phi_T{}^k\right) \cdot \right. \\ &\qquad \left. e^{-j\beta s^k} \cdot A_k\left(S_l^k, l = 0, 1, 2, \ldots, N_{EV}^k\right) \right\} \end{aligned} \quad (1)$$

where N_R is the number of rays, N_{EV}^k is the number of interactions experienced by the k-th ray, S_l^k is the length of the l-th segment composing the k-th path, $S^k = \sum_l S_l{}^k$ is the total, unfolded length of the k-th ray, $\mathbf{C}_l$ is an appropriate dyadic coefficient to properly decompose the incident field into orthogonal polarizations at the l-th interaction point, and includes the interaction coefficients (reflection coefficients, diffraction coefficients, etc.), $\mathbf{E}_{T0}^k$ is the field at a reference distance of 1 m from the Tx in the direction of departure $(\theta_T{}^k, \phi_T{}^k)$ of the k-th ray, $e^{-j\beta s^k}$ is the phase factor, and finally A_k represents the overall *divergence factor* of the k-th ray [22].

In the present work the 3D ray-tracing tool has been validated against mm-waves multidimensional measurements in the ''small-office'' scenario (Figure 2). RT simulation has been performed in all cases with a maximum of 3 reflections, single-bounce diffuse scattering (as either the first or the last interaction), single diffraction and transmission enabled for some of the internal objects (e.g. furniture). This combination of interactions has been found to be the best compromise between accuracy of the results and low CPU time.

The electromagnetic material characteristics (complex permittivity, ε_c) and the values of the scattering coefficient S are also important input parameters. While ε_c values at 60 GHz are available in the literature [24], the optimal S values have not been determined so far. Since S^2 defines the fraction of power diverted from specular reflection into diffuse scattering, the use of a correct value for S is very important as rough surface scattering is expected to be relevant due to the small wavelength. To determine the optimum S value, S has been varied from 0.4 (typical value for UHF frequencies) to 0.9 and the corresponding predictions have been compared with measurements in terms of Delay Spread (DS) (Figure 4) and the RMS error of Power-Angle-Spectrum (PAS) for the DoD (Figure 5), with the DS defined as follows:

$$DS = \sqrt{\sum_{i=1}^{N} (t_i - TM_0)^2 \cdot p_i} \quad (2)$$

with:

$$p_i = \frac{\rho_i^2}{P_{TOT}} = \frac{\rho_i^2}{\sum_{i=1}^{N} \rho_i^2}; \quad TM_0 = \sum_{i=1}^{N} t_i \cdot p_i \quad (3)$$

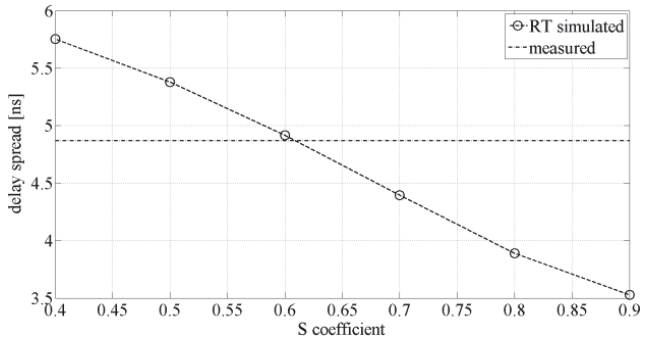

FIGURE 4. Comparison between measured and simulated delay spread for different values of the scattering coefficient S.

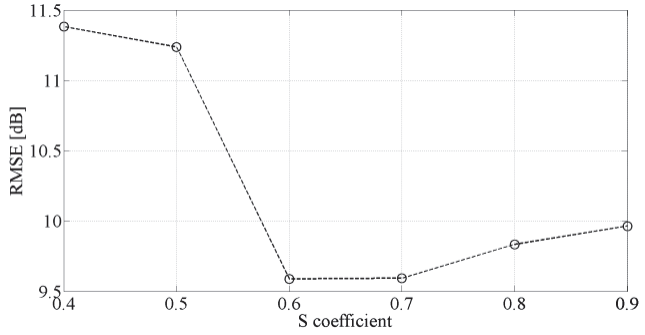

FIGURE 5. RMSE error of the difference between measured and simulated DOD-PAS for different values of the scattering coefficient S.

where ρ_i is the current or voltage signal amplitude at the Rx antenna port generated by the i-th incoming ray.

As shown in Figure 4, DS decreases with S: this can be explained considering that the shortest delay contributions are diffused for the considered Non-LOS (NLOS) Rx position, and their intensities increase with S. The best S value to reproduce the measured DS is S=0.6, which is also the most suitable value in terms of RMSE of the DOD-PAS (Figure 5).

The measured vs. simulated DOD-PAS's are compared for S=0.6 in Figure 6. It is evident that some strong contributions are missing in the upper left side of the simulated plot. These contributions probably correspond to specular reflections from the lamp on the ceiling and/or the frame of the windows, which were roughly included in the digital map, and therefore

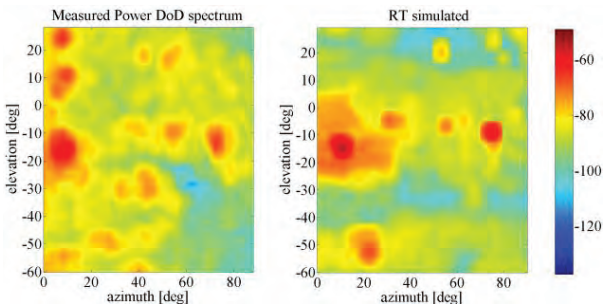

FIGURE 6. Measured and simulated DOD-PAS for S=0.6.

they are hardly visible in the simulated result. Even small objects, such as the mentioned lamp and frame, seem to have an important role at mm-wave frequencies. Therefore an accurate characterization of back-scattering from most common objects would be very useful. Overall, the PAS appear characterized by a few strong dominant paths or path clusters and by a low dense multipath component background, probably due to rough-surface scattering: propagation appears therefore quite suitable for pencil-beam forming transmission techniques.

III. RT-BASED EVALUATION OF DIFFERENT BEAMFORMING STRATEGIES

The tiny wavelength of mm-waves allows the use of a large number of radiating elements, often arranged in linear or planar array, to be hosted even in small, mobile/portable devices. This fact paves the way to BF solutions, where the power at the Tx side is kept focused around a given direction through a proper vector of "complex steering coefficients" (or "beamforming weights") applied to the signals transmitted by the radiating elements. A similar "steering vector" can be also applied at the Rx side to profitably shape the Rx pattern [25]. In order to reduce interference in a multi-user scenario, null-steering in addition to (or instead of) beam shaping may also represent a further option [26].

In addition to traditional single-beam steering techniques (single BF), multi-beam solutions (multi BF) can be also realized, where the signal is simultaneously delivered to the intended user through multiple radiation lobes. In order to mitigate the self-interference at the Rx between the different replicas of the signal transmitted and/or received through the multi-beam radiation pattern, some kind of re-alignment in time and co-phasing (i.e. equalization) is necessary.

BF effectiveness clearly increases with frequency, together with the feasibility of large-size arrays corresponding to narrow radiation beams, and therefore to greater spatial reuse factors and antenna gains.

Given the key role played by BF in future mm-waves radio systems, different BF solutions are considered and compared in this section on the base of RT simulations at 60 GHz, using the parameters defined in section II.B in the test environment represented in Figure 7. It is an indoor scenario made of a corridor with an Access Point (AP) and offices on a side, furnished with some objects such as wooden desks and metal cupboards. Internal walls are made of thin-plasterboard so that the signal can propagate into the offices, but metal cupboards randomly placed against the walls create strong NLOS conditions in several spots. The AP (Tx) is mounted on the ceiling and oriented at 45° toward the offices, whereas 24 Rx locations per cell are deployed on a grid as shown in Figure 7. Also similar cells in the upper and lower floor are considered, and adjacent cells on the same floor are taken into account in some cases for single-BF assessments (3 cells per floor, section IV.A) to simulate a large indoor environment with a high interference level.

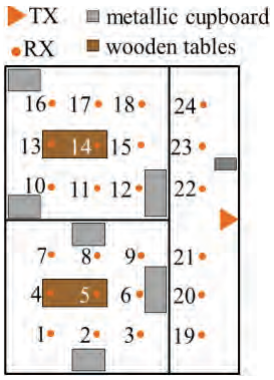

FIGURE 7. Example of 2D map considered for BF assessment (single cell per floor case).

The transmitting antenna is a 2×8 or a 12×12 planar array of patch radiators, transmitting an overall EIRP of 40 dBm, compliant with the power limit fixed by most of the current international regulations [27], [28]. Omnidirectional antennas are considered at the Rx.

In order to investigate the statistical properties of the Carrier to Interference plus Noise Ratio (CINR), one or two Rx's per cell have been considered, and for each position of the *user* the *interferer* has been moved over all the remaining locations. Multiple realizations of the whole process, depending on the number of considered cells, are taken into account according to a static, snap-shot simulation approach. For each simulation with 1 user per cell $24 \times N$ realizations have been considered, where N (typically N=10) is the number of different dispositions of one interferer per cell in the adjacent cells. For each simulation with 2 users per cell $24 \times 24 \times N$ realizations have been considered, where N is the number of different dispositions of two interferers per cell in the adjacent cells, see scheme in Figure 8.

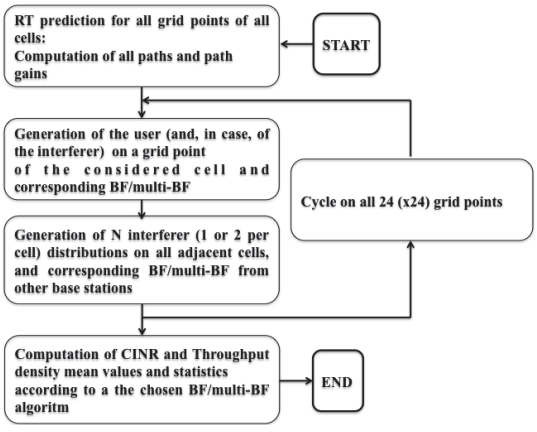

FIGURE 8. Space-division multi-user BF system simulation scheme.

Three major BF solutions have been investigated, namely:

1) *Radial BF*: assuming perfect localization available for each (Tx, Rx) pair, a radiation pattern with a single beam steered towards the radial direction Tx-Rx (irrespective of the presence of possible obstruction) is considered at the Tx array.
2) *Single BF*: the M strongest paths (with M = 6 here) are determined through RT simulation with isotropic antennas, then the Tx beam is steered toward the one of them yielding the best CINR value at the user.
3) *Multi BF*: the M strongest paths are determined through RT. Then, M beams are simultaneously generated and equalized in time and phase in order to focus the power at the Rx position and at the same time realize a sort of space diversity over different paths. In particular, this multi BF solution has been considered with M = 2 (Figure 9) and M = 4.

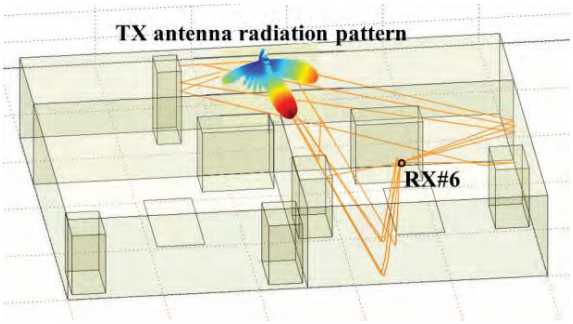

FIGURE 9. Example of dual beamforming, with the radiation lobes steered in the direction of departure of the two strongest paths.

It's worth noticing that radial BF doesn't actually involve any channel state sensing or prediction, since it just requires the knowledge of the Rx position and orientation. It is therefore simpler than the single/multi BF, but also rougher, as steering the beam towards the Rx location is of course ineffective in strongly NLOS cases.

IV. RESULTS

A. SINGLE BEAMFORMING

Simulation results of Figure 10 show the RT-simulated mean CINR in two extreme cases: a low interference (single-cell-per-floor, single-user) case where interference only comes from neighboring floors, and a high-interference case with 3 cells per floor and two space-divided users per cell.

Low-interference case results show that the single BF technique described in section III allows a CINR increase of up to 30 dB with respect to radial BF in NLOS Rx locations (e.g. locations # 2, 6, 7, 10, etc.) using the 2×8 array, and the increase is even greater for the 12×12 array. The use of an omnidirectional antenna at the AP (SISO case, just for reference here) of course yields a very poor CINR as no space division to separate user and interferers is possible in this case, although SISO performance is similar or even better than radial BF in NLOS locations.

Results are not that good in the high-interference case, especially for the 2×8 array, where BF spatial resolution is not able to single out and address "useful" paths due to the high number of interfering paths.

Throughput density results are shown in Figure 11, where throughput density (bit/s/Hz/m^2) has been computed

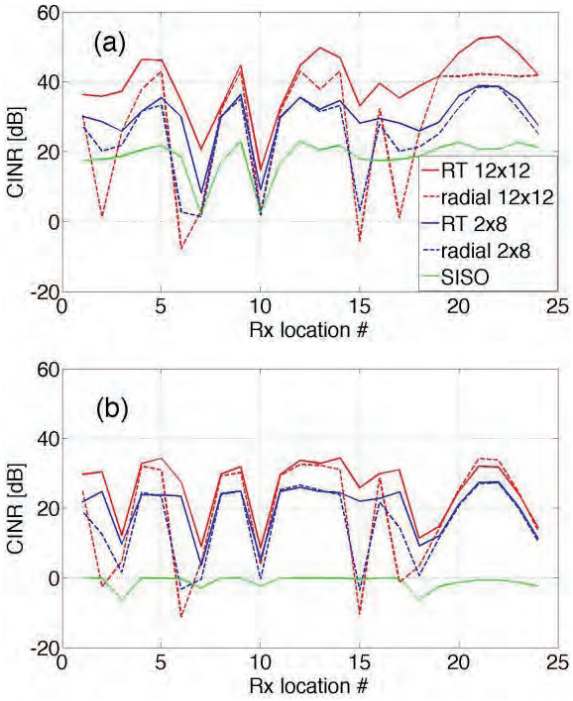

FIGURE 10. Mean CINR values for different Rx (user) locations and single-BF solutions. (a) 1cell per floor; 1user per cell; (b) 3 cells per floor; 2 users per cell.

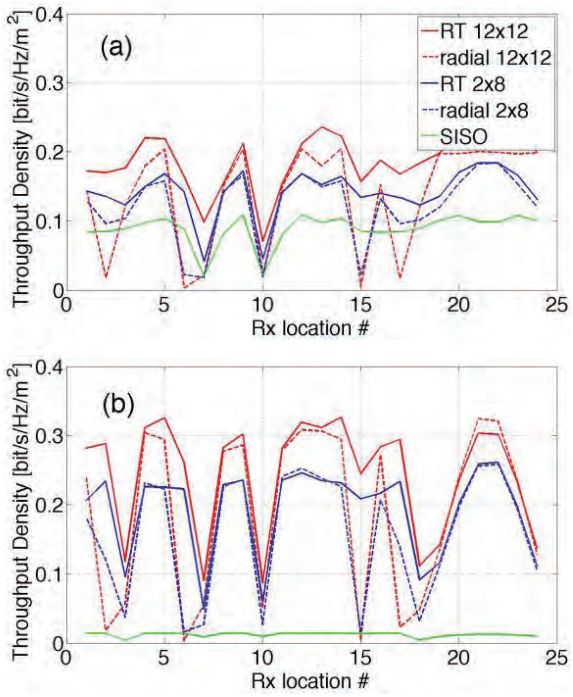

FIGURE 11. Mean Throughput Density for different Rx (user) locations and single-BF solutions. (a) 1cell per floor; 1user per cell; (b) 3 cells per floor; 2 users per cell.

considering the CINR, computing the channel's capacity through the Shannon-Hartley formula and multiplying the resulting figure by user density (users/m^2). Figure 11, lower graph, shows that throughput density values for the high-interference case are still comparable to or better than those of the low-interference case (upper graph) due to the greater user density made possible by intra-cell space division.

The CINR Cumulative Density Function (CDF) for the 1 cell per floor, 2 users per cell case, 12 × 12 array – the same case considered in the following section IV.B - is shown in Figure 12. The great advantage of taking into account the actual directional characteristics of the multipath channel is evident, especially for low CINR values – i.e. when a gain is needed the most – where RT-assisted BF achieves a gain of 20 to 30 dB with respect to radial BF.

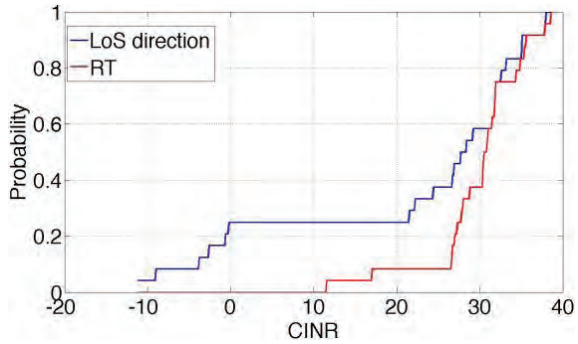

FIGURE 12. CINR Cumulative Density Function (CDF): single BF, 1 cell per floor; 2 users per cell; 12 × 12 array.

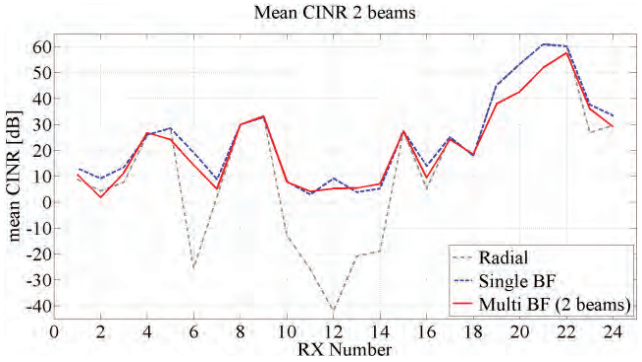

FIGURE 13. CINR values for different Rx locations and BF solutions – 1 cell per floor, 2 users per cell.

B. MULTI-BEAMFORMING

In Figure 13 the mean value of the CINR for each of the 24 locations is reported for the three BF techniques. As can be noticed performance is strongly location-dependent, since multipath and propagation is strictly related to the position of the receiver in the specific environment. The radial BF strategy of course poorly performs for NLOS receivers, while the single BF is the best solution in most cases.

The reason why the single BF is the most efficient solution can be explained by observing results in Figure 14, where the cumulative distribution of the difference of ray intensity of the 1st (strongest) path with respect to the 2nd strongest, the 3rd strongest and the 4th strongest is plotted. The difference between the intensity of the 1st and the 2nd path is greater than 5 dB in 70% of cases, which means that in the considered environment there is always a dominant path

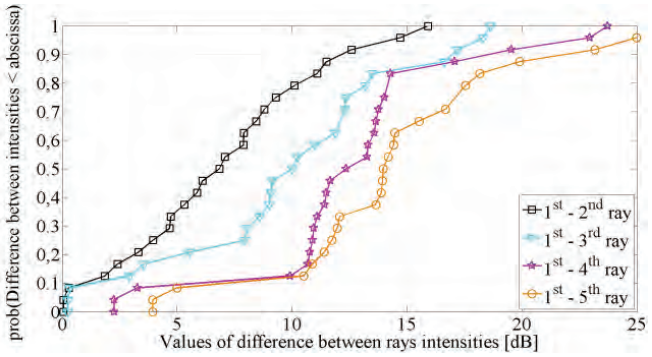

FIGURE 14. CDFs of the difference between the rays intensity.

towards which all the available power for transmission should be directed. This consideration is valid in general for all office-like environments with plasterboard walls. There are however cases (Rx # 4, 9, 11, 13, 14 in Figure 13) where the ray intensities of the two main paths are more uniform, and in this latter case the multi BF outperforms the single BF.

Performance of multi-BF downgrades if it's implemented with 4 beams, in particular if the power is uniformly distributed over all beams (Figure 15, center). This behavior is due to the fast reduction of the ray intensity with the increasing order of rays (Figure 14), therefore the radiated power in the direction of the 3rd and of the 4th ray is basically wasted in most cases.

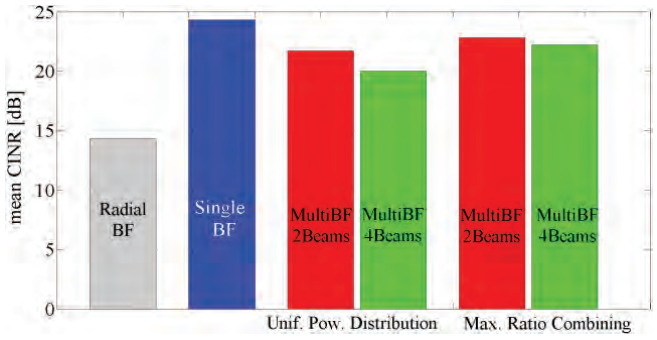

FIGURE 15. Mean CINR values for the considered BF solutions and for different power unbalance between the lobes in the multi BF case.

In order to limit power waste toward ''useless directions'', a non-uniform distribution of power can be implemented. In Figure 15, right side, the latter solution is shown and the average value of CINR is reported, corresponding to a transmitted power for each beam proportional to the associated path gain (in accordance with the Maximal Ratio Combining (MRC) algorithm [29]). Results show the improvement of the MRC solution with respect to the uniform power distribution (red and green bar chart, left and right in Figure 15).

Simulations shown in Figure 13 through Figure 15 are all in static conditions, i.e. no mobility inside the propagation environment is taken into account. Nevertheless, people may move indoors, and therefore dynamic, temporary partial/total obstruction of the rays may occur. In order to estimate the robustness of the considered BF solution to sudden, unexpected blockage, an additional loss of 30 dB (representative of full human blockage [30]) has been added on the main radiation lobe. As shown in Figure 16 the mean CINR value decreases for all the solutions, but the reduction is about 6 dB less severe for multi-BF with respect to single BF. Of course this is due to the intrinsic spatial diversity gain of the multi-BF schemes. Moreover, the more uniform the power distribution among the beams, the larger the diversity gain and the stronger system robustness to blockage impairment. In particular the reduction of the mean CINR for a two-beam multi BF case with uniform distribution of power is equal to 12 dB (not shown in Figure 16 for legibility), while it is equal to 16 dB for the MRC power distribution.

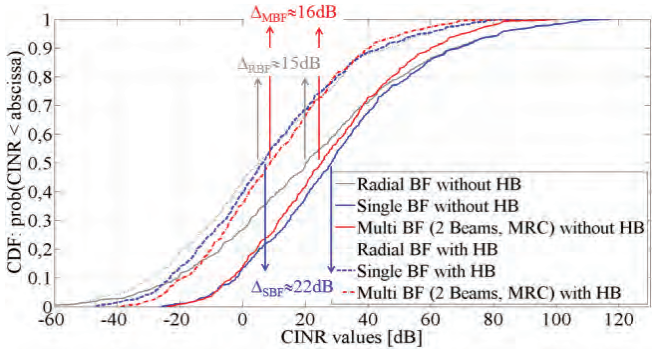

FIGURE 16. Impact of Human Blockage (HB) on different BF strategies.

In conclusion there is a trade-off between performance in static conditions, which would benefit from uneven power distribution among beams, and the capability to cope with sudden unpredictable link obstruction, which would require a more uniform power distribution.

The simple, radial solution is more insensitive to possible, dynamic obstruction of the radial path than single BF ($\Delta_{RBF} = 15$ dB vs. $\Delta_{SBF} = 22$ dB in Figure 16). This can be explained considering that the additional human blockage loss is a real impairment only when the radial path is in LOS conditions, otherwise the latter extra attenuation is not relevant. On the other hand human blockage always produces a strong reduction of received power in all cases for the single BF solution, as the beam is directed to the stronger path.

V. RAY TRACING ASSISTED BEAMFORMING FOR FUTURE GIGABIT WIRELESS SYSTEMS

A. BEAM-TRACKING ALGORITHM

BF at mm-waves can be carried out on the base of two different approaches, referred to as the ''fully adaptive'' and the ''switched'' case [12]. A fully adaptive array represent the most versatile solution, since it's able – at least in principle – to steer the beam in every direction, i.e. it can synthetize an unlimited number of radiation patterns. For each required orientation, the BF weights to be adopted are determined at the end of a tracking (or training) phase, when Channel State Estimation (CSE), i.e. some knowledge of the channel

matrix H, is acquired [12]. The CSE can be carried out according to some different procedures [12], [31] whose complexity and computational burden generally increases with the array dimension [32]. Therefore, the fully adaptive approach is often discarded in favor of the switched array solution, which is on the contrary based on a finite set of fixed, predefined patterns. The BF vectors corresponding to the available patterns are collected in a codebook [12], and the tracking phase basically consists of a somehow brute-force search of the best BF vector among those included in the codebook at the Tx and / or at the Rx side. The execution time required by a codebook-based BF algorithm depends on the codebook size and can become quite large when beams are very narrow and/or a beam scanning over a wide 3D range must be pursued.

Irrespective of the specific implementation, a codebook-based beam-tracking algorithm can be expected to perform well in static condition, where it should run just once at radio link set up. On the contrary, some doubts may arise about its effectiveness in a time variant channel. For instance, in large and crowded scenarios where moving people or other moving objects may suddenly block paths, the CINR value might drop (especially in the single BF case), thus triggering a new beam-tracking phase. In presence of frequent and unpredictable blocking occurrence, the tracking algorithm should be run over and over again, to the detriment of the overall system performance.

B. REAL TIME RT TECHNIQUE FOR ADVANCED BEAM TRACKING

The BF strategies introduced in section III and then evaluated in section IV clearly assume a thorough knowledge of the directional characteristics of the radio channel, as well as the awareness of the position of the devices. These information are commonly not easily available in modern wireless network but they are likely to be more and more accessible in the near future, thanks to the ongoing technological progresses (environment digitalization, powerful computing capabilities, sensing and localization techniques). This might open up new prospects, where radio channel models such as RT could be embedded into the radio devices and the BF process could be somehow piloted (totally or in part) in real time by the deterministic prediction.

It's worth noticing that RT-based beam tracking could naturally cope with fast and sudden channel changes (e.g. abrupt human blockage), because once the stronger paths have been tracked by the RT engine, their DoD could be easily stored, so that the beam(s) could be quickly re-arranged if needed.

Moreover, RT-assisted BF could be even faster than standard BF solutions, provided that the paths tracking time in the RT tool is lower than (or at least comparable to) the average time interval necessary to complete the exhaustive search inside the codebook.

In order to perform a preliminary comparison, the computation time required by RT simulations for the small office environment described in section II are shown in the following Table 1. Since the mm-wave channel is basically LOS or quasi-LOS with few dominant paths, RT simulation has been limited here to two reflections at most.

TABLE 1. RT simulation CPU time for the "small office" environment.

Interactions	Computation time (ms)
1 refl., 0 transm.	12
1 refl., 1 transm.	16
2 refl., 0 transm.	220
2 refl., 1 transm.	225

Computation time refers to a standard 2 GHz personal computer CPU. However a drastic reduction up to two orders of magnitude in CPU time can be achieved by properly parallelizing the algorithm and exploiting Graphical Processing Units available in today's and tomorrow's mobile devices.

Since BF at mm-waves is not yet widely used in currently operating networks, reliable on-field evaluation of the performance of standard, codebook-based beam-tracking algorithm are not easily available. A mm-wave BF prototype for 5G wireless systems is described in [33] and according to some tests the beam searching time has been estimated equal to 45 msec. Nevertheless, the beam scanning range has been limited to 60 degree in the horizontal plane and the Half Power Beam Width (HPBW) is equal to about 10 degree for each radiation pattern. Therefore, it can be somehow argued that in case of a full 3D scanning carried out with very narrow pencil-beams (i.e. HPBW of few degrees) the beamforming time could rise up to some hundreds of msec, not to mention the multi-BF case.

Although further investigations are necessary, this preliminary assessment might suggest that real time, RT-assisted BF is a promising technique that deserves consideration.

VI. CONCLUSIONS

In this work a full-3D Ray Tracing simulator is used as a tool to investigate advanced pencil-beam forming techniques in terms of carrier-to-interference plus noise ratio and throughput-density in a reference indoor multi-user environment, where different communications are assumed to be divided through space-division only.

Fully-adaptive beamforming and multi-beamforming strategies are considered that will become possible in the future, thanks to the availability of accurate localization, sensing and ray-based mm-wave propagation prediction tools.

Results show that "intelligent" fully-adaptive beamforming strategies can achieve good performance without any other division technique and can outperform simpler radial-beamforming techniques. Multi-beamforming is shown to perform almost as well as single-beamforming and in addition to yield a space (or angle) diversity gain of up to 10 dB in case of human blockage of the dominant path.

Ray tracing itself is also proposed and evaluated as a real-time prediction tool to assist future beamforming strategies,

and future promising applications are envisioned. This, and other aspects will be object of further investigations.

REFERENCES

[1] (Nov. 2013). *ERICSSON Mobility Report*. [Online]. Available: http://www.ericsson.com/mobility-report

[2] C. J. Hansen, "WiGiG: Multi-gigabit wireless communications in the 60 GHz band," *IEEE Trans. Wireless Commun.*, vol. 18, no. 6, pp. 6–7, Dec. 2011.

[3] M. Coldrey, J.-E. Berg, L. Manholm, C. Larsson, and J. Hansryd, "Non-line-of-sight small cell backhauling using microwave technology," *IEEE Commun. Mag.*, vol. 51, no. 9, pp. 78–84, Sep. 2013.

[4] T. S. Rappaport *et al.*, "Millimeter wave mobile communications for 5G cellular: It will work!" *IEEE Access*, vol. 1, pp. 335–349, May 2013.

[5] C. Gustafson, K. Haneda, S. Wyne, and F. Tufvesson, "On mm-wave multipath clustering and channel modeling," *IEEE Trans. Antennas Propag.*, vol. 62, no. 3, pp. 1445–1455, Mar. 2014.

[6] D. Dupleich *et al.*, "Directional characterization of the 60 GHz indoor-office channel," in *Proc. 31st URSI General Assembly Sci. Symp.*, Beijing, China, Aug. 2014, pp. 1–4.

[7] A. Paulraj, R. Nabar, and D. Gore, *Introduction to Space-Time Wireless Communications*. Cambridge, U.K.: Cambridge Univ. Press, May 2003.

[8] M. A. Jensen, Y. Shi, and Y. Yang, "Channel covariance modeling for multi-user MIMO systems," in *Proc. 4th Eur. Conf. Antennas Propag. (EuCAP)*, Barcelona, Spain, Apr. 2010, pp. 1–5.

[9] *IEEE Standard for Information Technology–Telecommunications and Information Exchange Between Systems–Local and Metropolitan Area Networks–Specific Requirements-Part 11: Wireless LAN Medium Access Control (MAC) and Physical Layer (PHY) Specifications Amendment 3: Enhancements for Very High Throughput in the 60 GHz Band*, IEEE Standard 802.11, Mar. 2014.

[10] *International Standard for Information Technology Telecommunications and Information Exchange Between Systems—Local and Metropolitan Area Networks—Specific Requirements. Part 15.3: Wireless Medium Access Control (MAC) and Physical Layer (PHY) Specifications for High Rate Wireless Personal Area Networks (WPANs)*, IEEE Standard 802.15.3c, 2009.

[11] B. Peng, S. Priebe, and T. Kurner, "Fast beam searching concept for indoor terahertz communications," in *Proc. 8th Eur. Conf. Antennas Propag. (EuCAP)*, The Hague, The Netherlands, Apr. 2014, pp. 639–643.

[12] S.-K. Yong, P. Xia, and A. Valdes-Garcia, *60GHz Technology for Gbps WLAN and WPAN: From Theory to Practice*. New York, NY, USA: Wiley, 2011.

[13] F. Fuschini, E. M. Vitucci, M. Barbiroli, G. Falciasecca, and V. Degli-Esposti, "Ray tracing for future small-cell and indoor applications: a review of current techniques," *Radio Sci.*, to be published.

[14] H. T. Friis, "A note on a simple transmission formula," *Proc. IRE*, vol. 34, no. 5, pp. 254–256, May 1946.

[15] K. Sato *et al.*, "Measurements of reflection and transmission characteristics of interior structures of office building in the 60-GHz band," *IEEE Trans. Antennas Propag.*, vol. 45, no. 12, pp. 1783–1792, Dec. 1997.

[16] G. Sommerkorn, M. Käske, C. Schneider, S. Häfner, and R. Thomä, "Full 3D MIMO channel sounding and characterization in an urban macro cell," in *Proc. 31st URSI General Assembly Sci. Symp.*, Beijing, China, Aug. 2014, pp. 1–4.

[17] R. Müller, R. Herrmann, D. A. Dupleich, C. Schneider, and R. S. Thoma, "Ultrawideband multichannel sounding for mm-wave," in *Proc. 8th Eur. Conf. Antennas Propag. (EuCAP)*, Apr. 2014, pp. 817–821.

[18] S. Wyne, K. Haneda, S. Ranvier, F. Tufvesson, and A. F. Molisch, "Beamforming effects on measured mm-wave channel characteristics," *IEEE Trans. Wireless Commun.*, vol. 10, no. 11, pp. 3553–3559, Nov. 2011.

[19] A. P. G. Ariza *et al.*, "60 GHz-ultrawideband real-time multi-antenna channel sounding for multi giga-bit/s access," in *Proc. IEEE 72nd Veh. Technol. Conf. Fall (VTC-Fall)*, Ottawa, ON, Canada, Sep. 2010, pp. 1–6.

[20] R. Zetik, M. Kmec, J. Sachs, and R. S. Thomä, "Real-time MIMO channel Sounder for emulation of distributed ultrawideband systems," *Int. J. Antennas Propag.*, vol. 2014, Sep. 2014, Art. ID 317683.

[21] R. G. Kouyoumjian and P. H. Pathak, "A uniform geometrical theory of diffraction for an edge in a perfectly conducting surface," *Proc. IEEE*, vol. 62, no. 11, pp. 1448–1461, Nov. 1974.

[22] V. Degli-Esposti, D. Guiducci, A. de'Mars, P. Azzi, and F. Fuschini, "An advanced field prediction model including diffuse scattering," *IEEE Trans. Antennas Propag.*, vol. 52, no. 7, pp. 1717–1728, Jul. 2004.

[23] V. Degli-Esposti, F. Fuschini, E. M. Vitucci, and G. Falciasecca, "Measurement and modelling of scattering from buildings," *IEEE Trans. Antennas Propag.*, vol. 55, no. 1, pp. 143–153, Jan. 2007.

[24] J. Lu, D. Steinbach, P. Cabrol, P. Pietraski, and R. V. Pragada, "Propagation characterization of an office building in the 60 GHz band," in *Proc. 8th Eur. Conf. Antennas Propag. (EuCAP)*, The Hague, The Netherlands, Apr. 2014, pp. 809–813.

[25] J. C. Liberti and T. S. Rappaport, *Smart Antennas for Wireless Communications*. Englewood Cliffs, NJ, USA: Prentice-Hall, 1999.

[26] M. Mouhamadou, P. Vaudon, and M. Rammal, "Smart antenna array patterns synthesis: Null steering and multi-user beamforming by phase control," in *Proc. Prog. Electromagn. Res. (PIER)*, vol. 60. 2006, pp. 95–106.

[27] *Broadband Radio Access Networks (BRAN); 60 GHz Multiple-Gigabit WAS/RLAN Systems; Harmonized EN Covering the Essential Requirements of Article 3.2 of the R&TTE Directive*, Standard ETSI EN 302 567, 2009.

[28] *Relating to the Use of Short Range Devices (SRD)*, document Rec. ERC 7003, Feb. 2014.

[29] A. Goldsmith, *Wireless Communications*. Cambridge, U.K.: Cambridge Univ. Press, 2005.

[30] M. Jacob *et al.*, "Fundamental analyses of 60 GHz human blockage," in *Proc. 7th Eur. Conf. Antennas Propag.*, Apr. 2013, pp. 117–121.

[31] L. Zhou and Y. Ohashi, "Efficient codebook-based MIMO beamforming for millimeter-wave WLANs," in *Proc. IEEE 23rd Int. Symp. Pers. Indoor Mobile Radio Commun. (PIMRC)*, Sep. 2012, pp. 1885–1889.

[32] P. Xia, S.-K. Yong, J. Oh, and C. Ngo, "Multi-stage iterative antenna training for millimeter wave communications," in *Proc. IEEE Global Telecommun. Conf.*, Nov./Dec. 2008, pp. 1–6.

[33] W. Roh *et al.*, "Millimeter-wave beamforming as an enabling technology for 5G cellular communications: Theoretical feasibility and prototype results," *IEEE Commun. Mag.*, vol. 52, no. 2, pp. 106–113, Feb. 2014.

VITTORIO DEGLI-ESPOSTI (M'94) received the Laurea (Hons.) degree and the Ph.D. degree in electronic engineering from the Università di Bologna, Bologna, Italy, in 1989 and 1994, respectively. From 1989 to 1990, he was with the Microwave Communications Group, Siemens Telecomunicazioni, Milan, Italy.

He has been with the Department of Electrical Engineering, Università di Bologna, since 1994, where he is currently an Associate Professor and teaches courses on electromagnetics, radio propagation, and wireless systems.

He was a Visiting Researcher with the NYU Polytechnic Institute, New York University, Brooklyn, NY, USA, in 1998. In 2006, he held a Visiting Professor position and taught the deterministic propagation modeling and ray tracing course at Aalto University, Espoo, Finland, and, in 2013, he held a Visiting Professor position at Tongji University, Shanghai, China. He still has ongoing research collaborations with the above-mentioned institutions, and several other universities and companies worldwide.

He participated in the European Cooperation Actions COST 231, COST 259, COST 273, COST 2100, and IC 1004, the European Networks of Excellence NEWCOM and NEWCOM++ in the European Project ALPHA, and several other national and international projects.

He has authored or co-authored about 100 peer-reviewed technical papers in the fields of applied electromagnetics, radio propagation, and wireless systems. He has been appointed as the Guest Editor of the IEEE Access online journal and serves as a reviewer for a number of IEEE Transactions journals.

He chaired, organized sessions, and served on the Technical Program Committees at several international conferences, including all EuCAP editions. He has been appointed as the Vice Chair of EuCAP2010 and EuCAP2011. He is an elected member of the Radio Propagation Board of the European Association on Antennas and Propagation.

He is a co-organizer and Lecturer with the European School of Antennas Course entitled Short Range Radio Propagation: Theory, Models and Future Applications.

Prof. Esposti has been elected as the Chair of the Cesena-Forli Unit of the Inter-Department Center for Industrial Research on ICT at the Università di Bologna in 2013.

FRANCO FUSCHINI was born in Bologna, Italy, in 1973. He received the degree (Hons.) in telecommunication engineering and the Ph.D. degree in electronics and computer science from the Università di Bologna, Bologna, in 1999 and 2003, respectively. He was a recipient of the Marconi Foundation Young Scientist Prize in the context of the XXV Marconi International Fellowship Award in 1999.

He held a post-doctoral position with the Department of Electronics and Computer Science, Università di Bologna, from 2004 to 2006. From 2007 to 2011, he was with the Marconi Wireless Consortium, Italy, where he served as a Research and Development Engineer in the areas of radio systems and wireless communications. He is currently a Research Associate with the Department of Electrical, Electronic and Information Engineering, Università di Bologna. He participated in the European Cooperation Actions COST 273, COST 2100, and IC 1004, the European Integrated Project FP7-ICT-ALPHA, and the European Networks of Excellence FP6-NEWCOM and FP7-NEWCOM++.

Dr. Fuschini's main research interests are in the area of radio systems design, and radio propagation channel theoretical modeling and experimental investigation.

ENRICO M. VITUCCI (S'04–M'08) received the M.Sc. degree in telecommunication engineering and the Ph.D. degree in electrical engineering and computer science from the Università di Bologna, Bologna, Italy, in 2003 and 2007, respectively. In 2007, he was a Visiting Researcher with Aalto University, Espoo, Finland. He is currently a Post-Doctoral Fellow with the Center of Industrial Research on ICT, Università di Bologna. His research interests are in mobile radio propagation, ray tracing models, MIMO channel modeling, and energy efficiency in urban areas. He participated in the European Cooperation Actions COST 273, COST 2100, and IC 1004, the European Networks of Excellence FP6-NEWCOM and FP7-NEWCOM++, and the European Integrated Project FP7-ICT-ALPHA. He has authored or co-authored over 30 technical papers in international journals and conferences. He also serves as a reviewer for a number of international journals, including several IEEE Transactions.

MARINA BARBIROLI received the Laurea degree in electronic engineering, and the Ph.D. degree in computer science and electronic engineering from the Università di Bologna, Bologna, Italy, in 1995 and 2000, respectively, where she has been a Researcher since 2001.

Her research interests are on propagation models for mobile communications systems, with a focus on the influence of the environment on signal fluctuations. Her research activities include investigation of planning strategies for mobile systems (GSM, UMTS, and LTE), broadcast systems (DVB-T and DVB H), and broadband wireless access systems (WiMAX and WiFi), and analysis of exposure levels generates by all wireless systems and study for compatibility trough different systems (broadcast systems and mobile communications systems) operating in the same band or in adjacent bands.

Dr. Barbiroli's research activity includes the participation to the European research and cooperation programs (COST 259, COST 273, COST 2100, and IC004) and the collaboration with Consorzio Elettra 2000 (formed by the Università di Bologna, Marconi Foundation, and Bordoni Foundation).

MARCO ZOLI received the B.Sc. degree in electronic and telecommunication engineering, and the M.Sc. degree in telecommunication engineering from the Università di Bologna, Bologna, Italy, in 2012 and 2014, respectively. He was a recipient of the Best Student Award in 2014 in the framework of the international master's degree course in Communications Networks, Systems, and Services. He is currently pursuing the Ph.D. degree in electronic, telecommunication, and information technologies with the Department of Electrical, Electronic, and Information Engineering, Università di Bologna. His main interests are radio channel modeling, ray tracing, beamforming and MIMO techniques, and millimeter-wave wireless systems.

LI TIAN (S'14) was born in Xiantao, China, in 1988. He received the bachelor's degree in communication engineering from Tongji University, Shanghai, China, in 2009.

He is currently pursuing the Ph.D. degree in control theory and control engineering with Tongji University. From 2013 to 2014, he was a visiting Ph.D. student with the Department of Electronics and Information Systems, Università di Bologna, Bologna, Italy. He participated in the 5G project sponsored by the National Natural Science Foundation of China. His current research interests are in the field of radio channel modeling and, in particular, propagation graph modeling, diffuse scattering models, and millimeter-wave channel modeling.

Mr. Tian serves as a reviewer for a number of international journals, including the IEEE Transactions on Vehicular Technology, the IEEE Antennas and Wireless Propagation Letters, and the *International Journal of Antennas and Propagation*

XUEFENG YIN received the B.S. degree in optoelectronics from the Huazhong University of Science and Technology, Wuhan, China, in 1995, the M.S. degree in digital communications and the Ph.D. degree in wireless communications from Aalborg University, Aalborg, Denmark, in 2002 and 2006, respectively. He is currently an Associate Professor with the College of Electronics and Information Engineering, Tongji University, Shanghai, China. His research interests are in sensor array signal processing, parameter estimation for radio channel, channel characterization and stochastic modeling, and channel simulation.

DIEGO ANDRES DUPLEICH received the Engineering degree in electronic engineering from the Universidad Tecnológica Nacional, Paraná, Argentina, in 2009, and the M.Sc. (Hons.) degree in communications and signal processing from the Ilmenau University of Technology, Ilmenau, Germany, in 2013, where he is currently pursuing the Dr.Ing. degree in electrical engineering.

He was a RF Specialist in Satellite Communications with Emerging Markets Communications, from 2009 to 2010. Since 2013, he has been with Prof. I. Thomä's research team and is currently working on the millimeter-wave field.

IEEE Access
The journal for rapid open access publishing

ROBERT MÜLLER received the M.S. degree in electronic engineering from the Berlin University of Technology, Berlin, Germany, in 2009. He is currently pursuing the Ph.D. degree with the Electronic Measurement Research Laboratory, Ilmenau University of Technology, Ilmenau, Germany. His areas of interest include high-frequency components design in Rogers and LTCC technology. Furthermore, he is also working on high-frequency front-end design, antenna design, ultrawideband system design, and special antenna array design for channel sounding applications. His research is focusing on channel sounding measurements system and analysis for further communication system in the field of V2V and cellular networks.

CHRISTIAN SCHNEIDER received the Diploma degree in electrical engineering from the Ilmenau University of Technology, Ilmenau, Germany, in 2001, where he is currently pursuing the Dr.Ing. degree with the Institute for Information Technology. His research interests include space-time signal processing, turbo techniques, adaptive techniques, multidimensional channel sounding, channel characterization and analysis, and channel modeling for single and multiuser cases in cellular and vehicular networks. He was a recipient of the Best Paper Award at the European Wireless Conference in 2013.

REINER S. THOMÄ (M92–SM99–F07) received the Dipl.-Ing. (M.S.E.E.), Dr.Ing. (Ph.D.E.E.), and Dr.Ing.Habil. degrees in electrical engineering and information technology from the Technical University of Ilmenau (TU Ilmenau), Ilmenau, Germany, in 1975, 1983, and 1989, respectively.

He was a Research Associate in the fields of electronic circuits, measurement engineering, and digital signal processing at TU Ilmenau from 1975 to 1988. From 1988 to 1990, he was a Research Engineer at the Zentrum für Wissenschaftlichen Gerätebau, Akademie der Wissenschaften der DDR. During this period, he worked in the field of radio surveillance. In 1991, he spent a three-month sabbatical leave at the Institute for Communications Engineering, University of Erlangen-Nuremberg, Erlangen, Germany. Since 1992, he has been a Professor of Electrical Engineering (Electronic Measurement) with TU Ilmenau, where he was the Director of the Institute of Communications and Measurement Engineering from 1999 to 2005. With his group, he has contributed to several European and German research projects and clusters such as RESCUE, WINNER, PULSERS, EUWB, NEWCOM, COST 273, COST 2100, IC 1004, EASY-A, and EASY-C. He was a speaker of the German nationwide DFG-focus project UKoLOS, Ultra-Wideband Radio Technologies for Communications, and Localization and Sensor Applications (SPP 1202). His research interests include measurement and digital signal processing methods (correlation and spectral analysis, system identification, sensor arrays, compressive sensing, and time-frequency and cyclostationary signal analysis), their application in mobile radio and radar systems [multidimensional channel sounding, propagation measurement and parameter estimation, and MIMO-wideband, millimeter-wave-wideband, and ultrawideband (UWB) radar], measurement-based performance evaluation of MIMO transmission systems, including over-the-air testing in virtual electromagnetic environments, and UWB sensor systems for object detection, tracking, and imaging.

Prof. Thomä is a member of URSI (Comm. A), VDE/ITG. Since 1999, he has served as the Chair of the IEEE-IM TC-13 on Measurement in Wireless and Telecommunications. He was a recipient of the Thuringian State Research Award for Applied Research both for contributions to high-resolution multidimensional channel sounding in 2007, and the Vodafone Innovation Award in 2014.